A Formulation of Radiation View Factors from Conical Surfaces

B.T.F. Chung,* M. M. Kermani,† and M.H.N. Naraghi‡
The University of Akron, Akron, Ohio

The purpose of this paper is to develop configuration factors from a cone or a truncated cone to a class of axisymmetric bodies such as a paraboloid, ellipsoid, or second conical surface. A closed-form solution for the view factor from a differential element to a circular cone is derived. Based on this formula, the view factors from a cone to a family of axisymmetric bodies are generated. The present approach leads to view factors that can be solved from a single numerical integration.

Nomenclature

a = focal length of paraboloid, half-length of major diameter of ellipsoid
A = surface area or a/r_c
b = half-length of minor diameter of ellipsoid
B = b/r_c
c = distance from origin to center of an ellipsoid
F = view factor
$f(x)$ = function generator of axisymmetric body
h = distance from element to the base of the cone (Fig. 1)
H = h/r_c
ℓ = length of the geometries
L = ℓ/r
n = unit normal vector from a differential element
p = distance between differential element and axis of the cone
P = p/r_c
r_c = radius of the base of a cone
s = distance between origin of the coordinates and tip of the cone (Fig. 1)
S = s/r_c
β = half-angle of the cone
θ = angle between n and z axis (Fig. 1)
ω = terminator angle defined by Eq. (1), (Fig. 1)

Subscripts

ax = axisymmetric body
c = cone
c_1 = cone 1
c_2 = cone 2
d = disk
dA_2 = differential element
e = ellipsoid
p = paraboloid
δ_r = differential conical ring

Introduction

THE determination of radiation view factor from a cone to an axisymmetric body is of practical importance in many engineering applications. Examples include radiative heat transfer between a spacecraft and its engine exhaust plume and radiation within internal engine cavities of a gas turbine cycle, since the exhaust plume and the engine cavity can be modeled as circular and truncated cone, respectively. Consequently, many attempts have been made by different investigators to determine the configuration factors from cones and frustum cones.

Campbell and McConnell[1] computed the view factor from cone to sphere by numerically integrating a complicated quadruple integral. Bobco[2] and Edwards[3] performed numerical integrations to determine the shape factor between a differential plane element and a conical frustrum. The Sparrow contour integral method[4] was employed by Holchendler and Laverty[5] and Minning[6] to evaluate the view factor from a differential area to a cone. Using Nusselt's double projection principle Morizumi[7,8] attempted to develop an analytical solution for the geometry factor between an elemental area and a cone. It is found that his formulation applies only to the case of a semi-infinite cone and the result is erroneous for the case of finite cone. Kobyshev et al.[9] studied the radiation between a cone and a coaxial disk that is in point contact with the cone. More recently, Chung and Naraghi[10,11] developed a much simpler formulation for the view factors from sphere and disk to a class of axisymmetric bodies, including the coaxial cone, sphere, etc. For further information on radiation view factor, the interested reader may refer to a recent publication of Howell.[12]

The present study continues previous efforts[10,11] and further develops the configuration factors from a cone or a truncated cone to a class of axisymmetric bodies such as a paraboloid, ellipsoid, or second conical surface. To facilitate the computations, a new analytical solution for the view factor from an arbitrary differential element to a circular cone is derived. Based on this formula, the view factors from a cone to a family of axisymmetric bodies are generated. Importantly, the present approach leads to a view factor that can be solved from a single numerical integration. To the best knowledge of the present authors, none of these results have previously appeared in the open literature.

Mathematical Analysis and General Formulation

In evaluating the shape factor between a cone and a coaxial axisymmetric body, a similar procedure presented in Refs. 10 and 11 will be adapted. It consists of three basic steps: 1) formulate the shape factor from an element to a cone using the contour integral method; 2) determine the view factor from a cone to a differential ring; 3) integrate the resulting expression from step 2 over the entire surface of the axisymmetric body.

Presented as Paper 83-0156 at the AIAA 21st Aerospace Sciences Meeting, Reno, Nev., Jan. 10-13, 1983; submitted March 4, 1983; revision submitted May 31, 1983.

*Professor, Department of Mechanical Engineering.
†Graduate Research Assistant, Department of Mechanical Engineering.
‡Research Associate, Department of Mechanical Engineering.

Shape Factor from an Arbitrary Differential Element to a Cone

We first determine what portion of the cone is visible by the element. The half angle of this portion of cone is defined as the terminator angle ω, which is given by Refs. 3 and 4 as

$$\omega = \cos^{-1}[-(s/p)\tan\beta] \tag{1}$$

Obviously the term inside the brackets cannot be greater than unity, i.e.,

$$|p| \geq |s\tan\beta|$$

The formulation of the view factor from dA_2 to the cone depends on whether the plane of dA_2 intersects the cone or not.

Case I

We first consider the case where the plane of dA_2 does not intersect the cone. The corresponding geometry is illustrated in Fig. 1. The shaded area of the cone is the portion visible by the element dA_2. The view factor F_{dA_2-c} can be obtained from the contour integral,

$$F_{dA_2-c} = \ell_2 \oint_c \frac{(z-z_2)\,dy-(y-y_2)\,dz}{2\pi L^2} + m_2 \oint_c \frac{(x-x_2)\,dz-(z-z_2)\,dx}{2\pi L^2} + n_2 \oint_c \frac{(y-y_2)\,dx-(x-x_2)\,dy}{2\pi L^2} \tag{2}$$

Now consider the differential element dA_2 in Fig. 1. The directions of the cosine of the element are $\ell_2 = 0$, $m_2 = \sin\theta$, and $n_2 = \cos\theta$; the coordinates of dA_2 are $x_2 = 0$, $y_2 = p$, and $z_2 = 0$. The contour of integration consists of the boundary line labeled 1, partial circumference of the cone base circle labeled 2, and another boundary line labeled 3, as shown in Fig. 1.

It is observed that great simplification can be made because of the symmetry of the contour about the z axis. Hence, the contour used here is line 1 and one-half of line 2.

By defining the radius of the cone as

$$\gamma = (z-s)\tan\beta \tag{3}$$

on boundary 1 we have

$$x = -\gamma\sin\omega, \quad y = \gamma\cos\omega, \quad z = \gamma\cot\beta + s \tag{4}$$

and

$$L^2 = \gamma^2\sec^2\beta - 2\gamma(p\cos\omega - s\cot\beta) + s^2 + p^2 \tag{5}$$

For boundary 2 we can write

$$x = r_c\sin\alpha, \quad y = r_c\cos\alpha, \quad z = h \tag{6}$$

and

$$L^2 = r_c^2 - 2pr_c\cos\alpha + p^2 + h^2 \tag{7}$$

The limits of the integration for boundary 1 are zero and r_c and for boundary 2 are $-\omega$ and zero.

Substituting the above expressions into Eqs. (2), carrying out the integration, and nondimensionalizing the result gives

$$F_{dA_2-c} = \frac{\sin\beta}{\pi P}(S\sin\theta + P\cos\theta)\cdot\left[\tan^{-1}\left(\frac{H}{\cos\beta\sqrt{P^2-S^2\tan^2\beta}}\right) - \tan^{-1}\left(\frac{S}{\cos\beta\sqrt{P^2-S^2\tan^2\beta}}\right)\right] + \frac{1}{\pi}\left(\frac{H}{P}\sin\theta + \cos\theta\right)$$
$$\times\tan^{-1}\sqrt{\frac{P+S\tan\beta}{P-S\tan\beta}} + \frac{1}{\pi}\left\{-\frac{H}{P}\sin\theta[(H-S)^2\tan^2\beta + P^2 + H^2] + \cos\theta[(H-S)^2\tan^2\beta - P^2 - H^2]\right\}$$
$$\times\frac{\tan^{-1}\sqrt{\dfrac{(H-S)^2\tan\beta + P^2 + H^2 + 2P(H-S)\tan\beta}{(H-S)^2\tan^2\beta + P^2 + H^2 - 2P(H-S)\tan\beta}\cdot\dfrac{P+S\tan\beta}{P-S\tan\beta}}}{\sqrt{[(H-S)^2\tan^2\beta + P^2 + H^2]^2 - 4P^2(H-S)^2\tan^2\beta}} \tag{8}$$

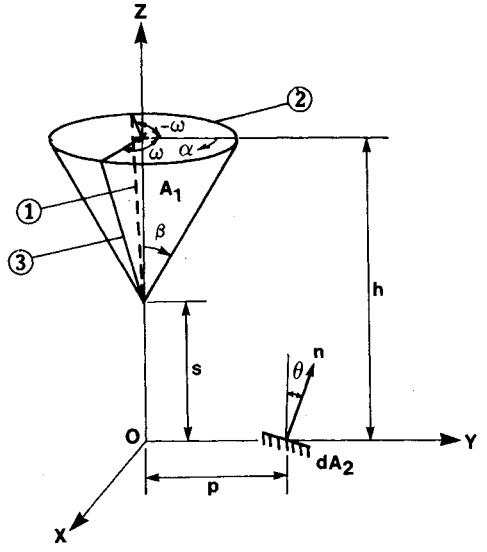

Fig. 1 Cone-differential element view factor geometry for case I.

where $0 \leq \theta \leq \tan^{-1}(S/P)$.

Case II

Figure 2 illustrates the second case for which the plane of dA_2 intersects the cone. Equation (2) still applies except that the contour of integration is different.

The intersection of the two surfaces is represented by GDE, which is a portion of perimeter of an ellipse. Integration of Eq. (2) along arc GDE introduces mathematical complexity such that the exact solution becomes extremely difficult, if not impossible. This is probably one of the reasons that no previous solution had been available for such problems. However, a closer examination reveals that the line integral over arc GDE is identical to that over straight line $\overline{GE}$, since dA_2 does not see the surface GDE. Thus, Eq. (2) is integrated along the contour formed by the path 1-2-3-4 instead of the path 1-2-3-4′. This simplification, in effect, reduces this problem to a case of radiation from the differential element dA_2 to the geometry EHCPG, as shown in Fig. 3.

Because of the symmetry of the geometry, only the half-contour path MEHNC is considered. For the line EH we have,

$$x=x,\ y=-x\cot\omega,\ z=s-x(h-s)/\tan\beta=s-x(\cot\beta/\sin\omega) \tag{9}$$

and

$$L^2=x^2\csc^2\omega\csc^2\beta-2xs\csc\omega\csc\beta\sec\beta+s^2+p^2 \tag{10}$$

From Fig. 3, we see that the lower limit of the integration for this boundary is the x coordinate of point E and the upper limit of integration is the x coordinate of point H as follows:

$$x_E=\frac{r_c(p\tan\theta-s)\sin\omega}{r_c\tan\theta\cos\omega+h-s},\qquad x_H=-r_c\sin\omega \tag{11}$$

Obviously, the boundary HC (or boundary 2 in Fig. 2) is the same as in case I as described by Eqs. (6) and (7). For boundary ME (or boundary 4 in Fig. 2) we have

$$x=x,\ y=\frac{r_c(p\tan\theta-s)\cos\omega}{r_c\tan\theta\cos\omega+h-s},\ z=\frac{\tan\theta[r_cs\cos\omega+p(h-s)]}{r_c\tan\theta\cos\omega+h-s} \tag{12}$$

and

$$L^2=x^2+\sec^2\theta\left[\frac{r_cs\cos\omega+p(h-s)}{r_c\tan\theta\cos\omega+h-s}\right]^2 \tag{13}$$

The lower limit of the integration of this portion of the contour is the x coordinate of point M, which is $x=0$. The upper limit of the integration is the x coordinate of point E given in Eq. (11).

Substituting the x, y, and z of different boundaries into Eq. (2) and performing the integrations yields the following closed-form solution for the view factor from a differential element to an intersected cone:

$$F_{dA_2-c}=\frac{1}{\pi}\tan^{-1}\left(\frac{\tan\beta(P\sin\theta-S\cos\theta)}{\sqrt{P^2-S^2\tan^2\beta}}\right)+\frac{\sin\beta}{\pi}\left(\frac{S}{P}\sin\theta+\cos\theta\right)\left\{\tan^{-1}\left[\frac{H}{\cos\beta\sqrt{P^2-S^2\tan^2\beta}}\right]\right.$$
$$\left.-\tan^{-1}\left[\frac{\tan\theta}{\cos\beta}\frac{\sqrt{P^2-S^2\tan^2\beta}}{P-S\tan^2\beta\tan\theta}\right]\right\}+\frac{1}{\pi}\left(\frac{H}{P}\sin\theta+\cos\theta\right)\tan^{-1}\sqrt{\frac{P+S\tan\beta}{P-S\tan\beta}}+\frac{1}{\pi}\left[((H-S)^2\tan^2\beta-P^2-H^2)\cos\theta\right.$$
$$\left.-\frac{H}{P}((H-S)^2\tan^2\beta+P^2+H^2))\sin\theta\right]\frac{\tan^{-1}\sqrt{\dfrac{(H-S)^2\tan^2\beta+P^2+H^2+2P(H-S)\tan\beta}{(H-S)^2\tan^2\beta+P^2+H^2-2P(H-S)\tan\beta}\cdot\dfrac{P+S\tan\beta}{P-S\tan\beta}}}{\sqrt{[(H-S)^2\tan^2\beta+P^2+H^2]^2-4P^2(H-S)^2\tan^2\beta}} \tag{14}$$

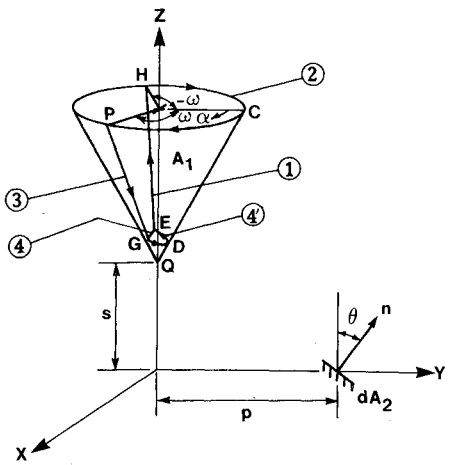

Fig. 2 Cone-differential element view factor geometry for case II.

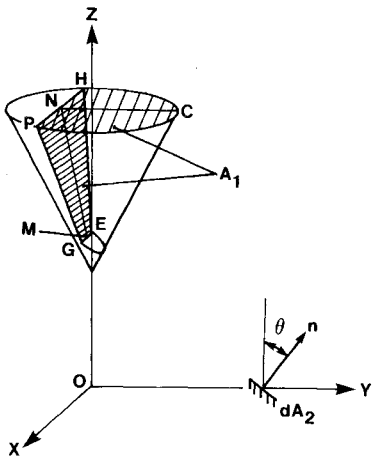

Fig. 3 The contour of the line integration along the cone.

where

$$\theta_1\le\theta\le\theta_2,\qquad \theta_1=\tan^{-1}(S/P)$$

and

$$\theta_2=\tan^{-1}\left(\frac{PH}{P^2+S(H-S)\tan^2\beta}\right)$$

The above inequality is an important criterion for the validity of Eq. (14).

The angles θ_1 and θ_2 are shown in Fig. 4. The above condition simply states that to use Eq. (14) the surface normal of the differential element must be between θ_1 and θ_2.

The reason for $\theta\ge\theta_1$ is rather obvious. Equation (14) is applied to the case of the intersection of the element with the cone. On the other hand, the reason for $\theta\le\theta_2$, may not be so obvious. Refer back to the line $\overline{GE}$ in Fig. 3. As the element is rotated in the direction of increasing θ the line GE moves toward line PN. When $\theta=\theta_2$ lines GE and PN coincide. But as $\theta>\theta_2$ the line GE falls above line PN. As one may recall, the coordinates of points G and E were the lower limits of integration and, once they fall above points P and N, the value of the integral becomes negative. Hence, Eq. (14) is no longer valid. For a special case of $\theta=0$, Eq. (8) is reduced to Eq. (8) of Ref. 6. Furthermore, if we set $\theta=0$ and S is replaced by $-S$, Eq. (14) becomes identical to Eq. (7) of Ref. 6.

The numerical results based on Eqs. (8) and (14) are illustrated in Fig. 5, for the case of $H=1$ and $\beta=30$ deg.

View Factor from a Cone to a Differential Conical Ring

Imagining that the differential element mentioned in the previous section is located on the outer surface of a differential conical ring, we now consider the radiation between this differential element and the cone shown in Fig. 6. By applying reciprocal rule, the view factor between cone and the

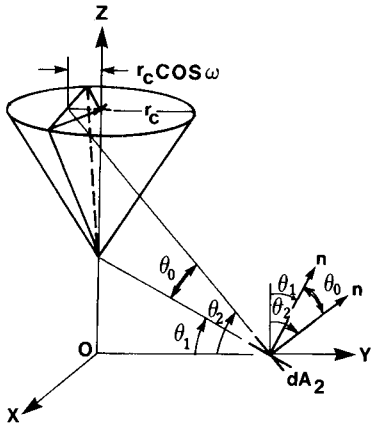

Fig. 4 Illustration of angles θ_1 and θ_2.

differential conical ring can be determined,

$$dF_{c-dA_2} = \frac{F_{dA_2-c}}{A_c} dA_2 \tag{15}$$

with

$$dA_2 = y d\phi d\ell \tag{16}$$

and

$$A_c = \pi r_c \sqrt{r_c^2 + \ell_c^2} \tag{17}$$

Substituting Eqs. (16) and (17) into Eq. (15) and integrating with respect to ϕ from zero to 2π, the view factor between a cone and a differential conical ring is obtained,

$$dF_{c-\delta r} = \int_0^{2\pi} \frac{y d\ell}{\pi r_c \sqrt{r_c^2 + \ell_c^2}} F_{dA_2-c} d\phi = \frac{2y}{r_c \sqrt{r_c^2 + \ell_c^2}} F_{dA_2-c} d\ell \tag{18}$$

where F_{dA_2-c} is given by Eqs. (8) and (14), respectively, depending upon whether the tangential plane of the element on the differential ring intersects the cone or not.

View Factor from the Cone to a Coaxial Axisymmetric Body

The differential ring mentioned in the previous section can be considered as a differential section of any axisymmetric geometry about the x axis. Let the function generator of this axisymmetric body be $f(x)$. We then have

$$d\ell = \sqrt{1 + [f'(x)]^2}\, dx \tag{19}$$

and

$$\theta = \cot^{-1}[f'(x)] \tag{20}$$

Combining Eqs. (8) and (18-20) and replacing s, p, and h in Eq. (8) by x, $f(x)$, and $(\ell_c + x)$, respectively, we arrive at the following expression for view factor from cone to a differential conical ring in terms of x, $f(x)$, and $f'(x)$:

$$dF_{c-\delta r} = \frac{2f(x)}{r_c\sqrt{r_c^2+\ell_c^2}} \left\{ \frac{\sin\beta}{\pi} \left[\frac{x + x[f'(x)]^2 + f(x)\cdot f'(x)}{f(x)\sqrt{1+[f'(x)]^2}} \right] \left(\tan^{-1}\left[\frac{\ell_c + x}{\cos\beta\sqrt{[f'(x)]^2 - x^2\tan^2\beta}} \right] \right.\right.$$

$$\left. - \tan^{-1}\left[\frac{x}{\cos\beta\sqrt{[f(x)]^2 - x^2\tan^2\beta}} \right] \right) + \frac{1}{\pi} \left(\frac{\ell_c + x + \ell_c\cdot[f'(x)]^2 + x[f'(x)]^2 + f(x)\cdot f'(x)}{f(x)\sqrt{1+[f'(x)]^2}} \right) \tan^{-1}\sqrt{\frac{f(x)+x\tan\beta}{f(x)-x\tan\beta}}$$

$$+ \frac{1}{\pi}\left[f'(x)\cdot f(x)\cdot(\ell_c^2\tan^2\beta - (\ell_c+x)^2 - [f(x)]^2) - (\ell_c+x)\cdot(\ell_c^2\tan^2\beta + [f(x)]^2 + (\ell_c+x)^2) \right]$$

$$\times \tan^{-1}\sqrt{\frac{\ell_c^2\tan^2\beta + [f(x)]^2 + (\ell_c+x)^2 + 2\ell_c f(x)\tan\beta}{\ell_c^2\tan^2\beta + [f(x)]^2 + (\ell_c+x)^2 - 2\ell_c f(x)\tan\beta}} \cdot \frac{f(x)+x\tan\beta}{f(x)-x\tan\beta}$$

$$\left. \div \{ f(x)\sqrt{1+[f'(x)]^2}\sqrt{[\ell_c^2\tan^2\beta + [f(x)]^2 + (\ell_c+x)^2\tan^2\beta]^2 - 4[f(x)]^2\ell_c^2\tan^2\beta} \} \right\} \sqrt{1+[f'(x)]^2}\, dx \tag{21a}$$

The above equation is applied to the case where the tangential plane of the differential ring does not intersect the cone.

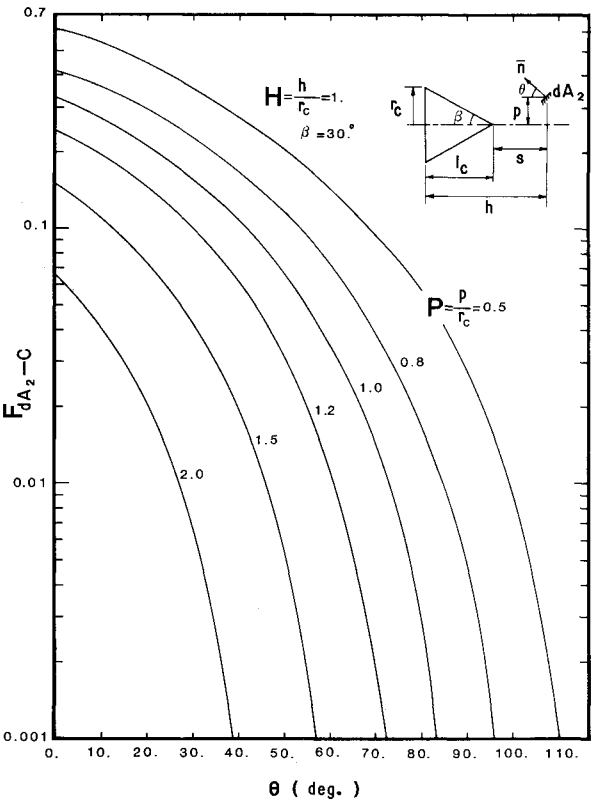

Fig. 5 Radiation view factor from a differential element dA_2 to a cone.

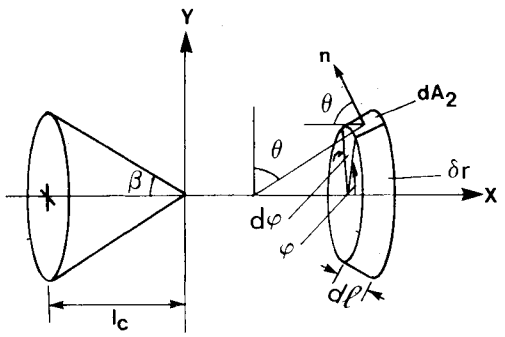

Fig. 6 Cone-coaxial differential conical ring view factor geometry.

Doing the same with Eq. (14) we obtain $dF_{c-\delta r}$ for the case where the tangential plane of the differential element intersects the cone,

$$dF_{c-\delta r}=\frac{2f(x)}{r_c\sqrt{r_c^2+\ell_c^2}}\left\{\frac{1}{\pi}\tan^{-1}\frac{[f(x)-xf'(x)]\tan\beta}{\sqrt{1+[f'(x)]^2}\cdot\sqrt{[f(x)]^2-x^2\tan\beta}}+\frac{\sin\beta}{\pi}\left(\frac{x+f(x)\cdot f'(x)}{f(x)\sqrt{1+[f'(x)]^2}}\right)\right.$$

$$\times\left\{\tan^{-1}\left[\frac{\ell_c+x}{\cos\beta\sqrt{[f(x)]^2-x^2\tan^2\beta}}\right]-\tan^{-1}\left[\frac{\sqrt{[f(x)]^2-x^2\tan^2\beta}}{[f(x)\cdot f'(x)-x\tan^2\beta)\cos\beta}\right]\right\}+\frac{1}{\pi}\left(\frac{\ell_c+x+f(x)\cdot f'(x)}{f(x)\sqrt{1+[f'(x)]^2}}\right)$$

$$\times\tan^{-1}\sqrt{\frac{f(x)+x\tan\beta}{f(x)-x\tan\beta}}+\frac{1}{\pi}[f(x)\cdot f'(x)(\ell_c^2\tan^2\beta-[f(x)]^2-(\ell_c+x)^2)-(\ell_c+x)(\ell_c^2\tan\beta+[f(x)]^2+(\ell_c+x)^2)]$$

$$\times\tan^{-1}\sqrt{\frac{\ell_c^2\tan^2\beta+[f(x)]^2+(\ell_c+x)^2+2\ell_c\tan\beta f(x)}{\ell_c^2\tan^2\beta+[f(x)]^2+(\ell_c+x)^2-2\ell_c\tan\beta f(x)}}\cdot\frac{f(x)+x\tan\beta}{f(x)-x\tan\beta}$$

$$\left.\div[f(x)\sqrt{1+[f'(x)]^2}\sqrt{[\ell_c^2\tan^2\beta+[f(x)]^2+(\ell_c+x)^2]^2-4\ell_c^2\tan^2\beta[f(x)]^2}]\right\}\sqrt{1+[f'(x)]^2}dx \tag{21b}$$

Integration of Eqs. (21) yields the shape factor from the cone to the axisymmetric body. However, special attention must be paid to the evaluation of the integration limits. In the case where the axisymmetric body does not intersect the cone, five different regions, in general, are recognized, as shown in Fig. 7. The view factor from the cone to an axisymmetric body shown in Fig. 7 is

$$F_{c-ax}=F_{c-I}+F_{c-II}+F_{c-III}+F_{c-IV} \tag{22}$$

In this figure all the points on region I, where $x_0\le x\le x_1$ can see the whole cone including the circumference of the base disk of the cone without any blockage. Hence, the view factor between this region an the cone is the same as that between region I and the base disk of the cone. The view factor from disk to this region is given in Ref. 11 as

$$F_{d-1}=\frac{1}{2r_c^2}\{[f(x_1)]^2+x_1^2+r_c^2$$

$$-\sqrt{\{r_c^2+[f(x_1)]^2+x_1^2\}^2-4[f(x_1)]^2r_c^2}\} \tag{23}$$

and by reciprocity we have

$$F_{c-I}=A_dF_{d-1}/A_c \tag{24}$$

On region II of the axisymmetric body with $x_1\le x\le x_2$, all the points see the cone completely and their tangential planes do not intersect the cone. In this case Eq. (21a) should be substituted for F_{dA_2-c} in Eq. (18). Integration of Eq. (18) from x_1 to x_2 yields the view factor between a cone and region II (a finite conical ring), i.e.,

$$F_{c-II}=\int_{x_1}^{x_2}dF_{c-\delta r}$$

On region III, where $x_2\le x\le x_3$, all of the point see the cone, but their tangential planes intersect the cone. Hence, to find the view factor from the cone to the region III of the axisymmetric body, Eq. (21b) is substituted into Eq. (18) and integrating it from x_2 to x_3 yields the shape factor from cone to a finite conical ring formed by region III, i.e.,

$$F_{c-III}=\int_{x_2}^{x_3}dF_{c-\delta r}$$

The region IV is equally as important as the previous regions. All the points in this region can see only a portion of the cone which can be treated as a portion of the base disk as far as irradiation is concerned.

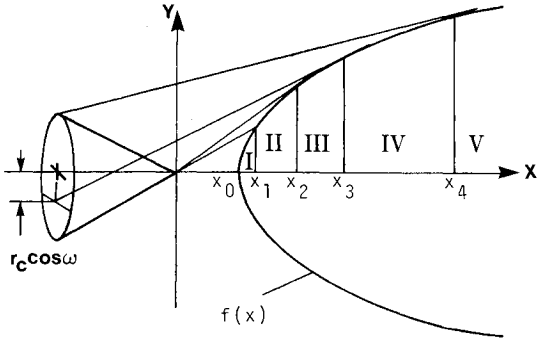

Fig. 7 Five regions of the axisymmetric body as viewed from a coaxial cone.

Therefore, for this case, the view factor between the axisymmetric body and the cone is the same as that in the case of an axisymmetric body and a portion of a disk. The view factor from a disk to region IV is given in Ref. 11 as

$$dF_{(d-\delta r)IV}=\frac{2}{\pi r_c^2}$$

$$\left\{\frac{-r_c^2[x-f'(x)\cdot f(x)]-[x+f'(x)\cdot f(x)](x^2+[f(x)]^2)}{\sqrt{r_c^4+2r_c^2(x^2-[f(x)]^2)+([f(x)]^2+x^2)^2}}\right.$$

$$\times\tan^{-1}\sqrt{\frac{[(r_c+f(x))^2+x^2][r_c+xf'(x)-f(x)]}{[(r_c+f(x))^2+x^2][r_c-xf'(x)+f(x)]}}$$

$$+\frac{1}{2}(x+f'(x)\cdot f(x))\cos^{-1}\left(\frac{f(x)-xf'(x)}{r_c}\right)$$

$$\left.+f(x)\sqrt{1+[f'(x)]^2}\cdot\tan^{-1}\left[\frac{\sqrt{(r_c^2-[xf'(x)-f(x)]^2}}{x\sqrt{1+[f'(x)]^2}}\right]\right\}dx \tag{25}$$

where $x_3\le x<x_4$.

Integrating Eq. (25) from x_3 to x_4 yields the configuration factor from the base disk to the conical ring of region IV, F_{d-IV}. From reciprocal rule, there is obtained

$$F_{c-IV}=A_dF_{d-IV}/A_c$$

The view factor from cone to the region IV is therefore obtained.

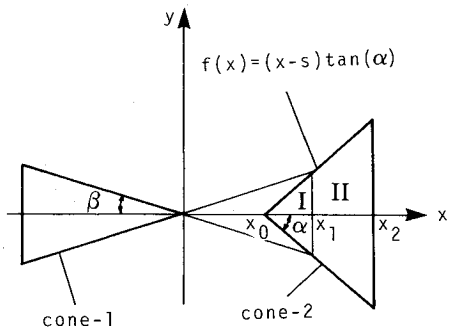

Fig. 8 Geometrical arrangement between two coaxial cones.

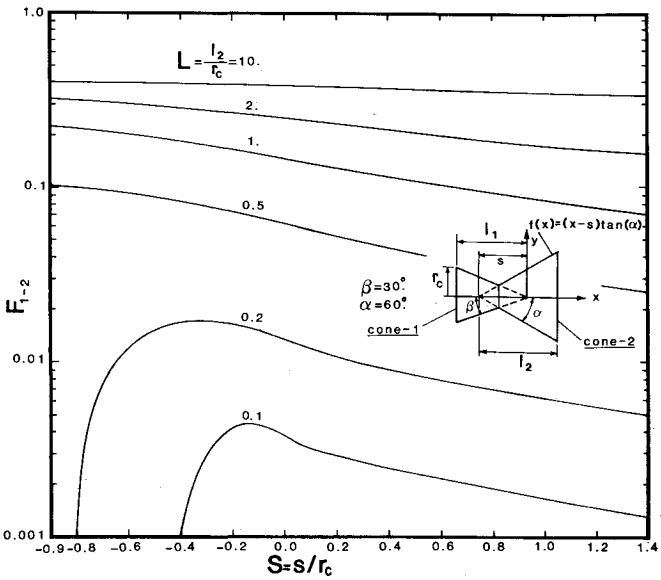

Fig. 9 View factor between two coaxial cones (F_{1-2} vs S with L as a parameter).

Region V corresponds to the surface area on the axisymmetric body that cannot be seen by the cone and hence does not contribute to view factor.

Substituting all the values of $F_{c-\mathrm{I}}$, $F_{c-\mathrm{II}}$, $F_{c-\mathrm{III}}$, and $F_{c-\mathrm{IV}}$ into Eq. (22), we arrive at the final result of geometric factor from cone to axisymmetric body, F_{c-ax}.

The following equations are utilized to solve for the integration limits x_0 to x_4:

$$f(x_0)=0 \tag{26}$$

$$f(x_1)-x_1\tan\beta=0 \tag{27}$$

$$f(x_2)-x_2f'(x_2)=0 \tag{28}$$

$$[f(x_3)]^2+x_3\ell_c\tan\beta-(x_3+\ell_c)f(x_3)\cdot f'(x_3)=0 \tag{29}$$

$$f(x_4)-\ell_c\tan\beta-(x_4+\ell_c)\cdot f'(x_4)=0 \tag{30}$$

It should be noted that not necessarily all axisymmetric bodies consist of all five regions mentioned above. For example, a cone consists of only two regions, namely regions I and II; further more, if the axisymmetric body is intersection with the cone, regions I and II do not exist.

Application and Results

As pointed out earlier, the present approach leads to a general expression for view factor that can be solved using a single numerical integration. A general computer program is developed to evaluate the factors numerically. In the program

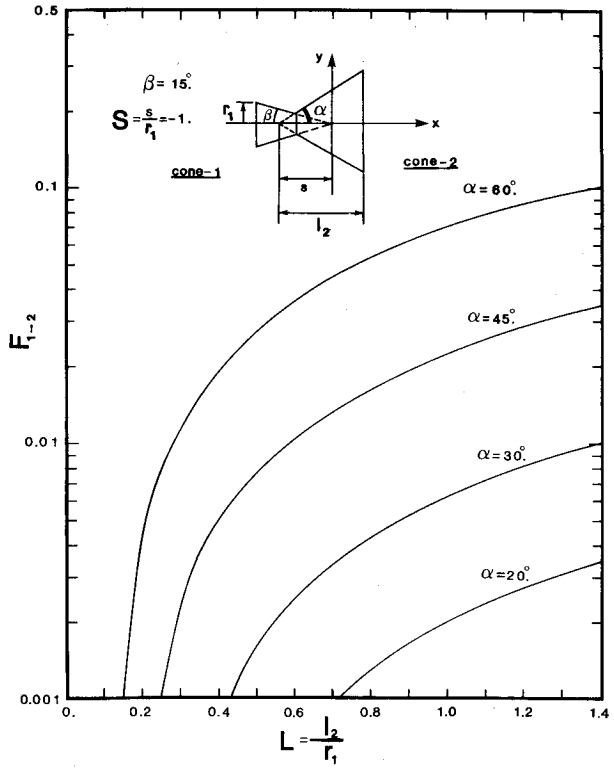

Fig. 10 View factor between two coaxial cones (F_{1-2} vs L with α as a parameter).

the 32-point Gauss quadrature technique with a double precision algorithm is employed to perform the integrations. To further check the validity of the present formulation and the accuracy of the numerical results, the view factor from a cone to a coaxial sphere was computed first as a benchmark. Note that the view factor from a sphere to a coaxial cone is available in Ref. 10. Numerical comparisons have shown that the agreement between two solutions is within six significant digits.

The same computer program was then used to generate shape factors from a cone or truncated cone to other axisymmetric bodies including an ellipsoid, a paraboloid, and a second cone or truncated cone. For convenience, the apex of the first cone c_1 (or the imaging apex of the truncated cone, see the sketch in Fig. 9) is always set at the origin of the coordinates. In the case when the cone and the axisymmetric body intersect, c_1 becomes a truncated cone and the axisymmetric body becomes a truncated axisymmetric body. Under this condition, the distance between the two bodies should be a negative value numerically.

We first consider the case of radiation between two nonintersecting cones with the location of the first cone being fixed. The function generator of the second cone is

$$f(x)=(x-s)\tan\alpha \tag{31}$$

Figure 8 illustrates the geometrical arrangement for this case. As can be seen this problem involves only regions I and II, as mentioned earlier. However, if the second cone is so short that $\ell_2 \le x_1$, even region II does not exist.

Assuming $\beta<\alpha$, the view factor from the cone to region I can be also obtained by considering radiation between the disk on the base of the cone with a smaller nose angle and the disk at x_1. The view factor from the cone to region II of the second cone is solved by integrating Eq. (21) from x_1 to x_2. If $\alpha<\beta$, the view factor from c_2 to c_1 is found first using the aforementioned approach and then the reciprocal rule is applied to give F_{1-2}.

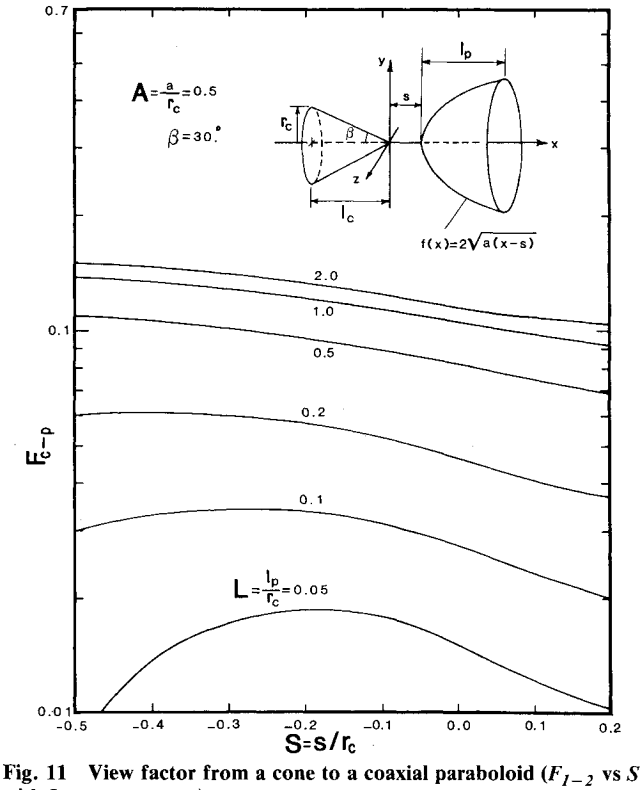

Fig. 11 View factor from a cone to a coaxial paraboloid (F_{1-2} vs S with L as a parameter).

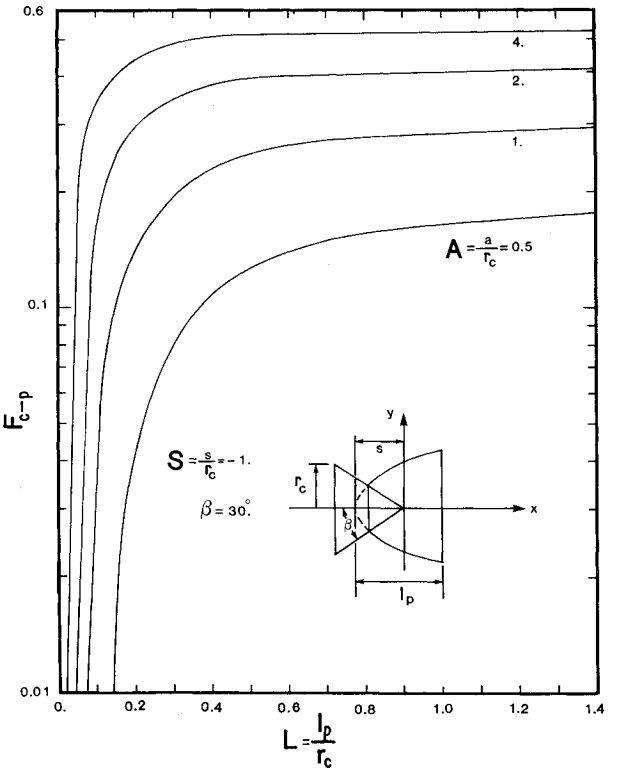

Fig. 12 View factor from a cone to a coaxial paraboloid (F_{c-p} vs L with A as a parameter).

For a fixed distance between two cones as the length of the second cone c_2 is increased, the view factor first increases rapidly and then approaches a limit asymptotically; but the view factor increases at a lower rate when two cones are rather apart.

Another interesting case is that when they are intersecting with each other both cones become truncated cones, as can be seen in the sketch of Fig. 9. Under this condition, only region II (see Fig. 7) exists. Figure 9 illustrates the variation of F_{1-2} as a function of distance between the cones (negative s), where the length of the moving cone c_2 is used as a parameter. It is observed that a maximum value of view factor exists for given ℓ_2. This maximum value always occurs at some location where the two cones are in interaction. The maximum location shifts to the left as the length of cone 2 increases. This information may be useful to optimize radiative exchange from conical surfaces.

Figure 10 demonstrates how the nose angle and the length of the second truncated cone affect the configuration factor. As expected, the view factor becomes less when α gets smaller if the length of cone 2 is fixed. This is mainly due to the fact that the surface area of cone 2 decreases as its angle is decreased and consequently the amount of incident energy decreases. For the same reason, the view factor decreases with the decrease of the length of the second truncated cone.

Consideration is now given to the situation where heat is transferred by radiation from a cone to a separated paraboloid. The function generator for a paraboloid is given by

$$f(x) = 2\sqrt{a(x-s)} \tag{32}$$

Unlike that from cone to cone, radiation from cone to paraboloid involves the four regions illustrated in Fig. 7 if the paraboloid is sufficiently long, i.e., $\ell_p \geq x_4$. The view factor from the cone to the paraboloid F_{c-p} is increased as the length of the paraboloid ℓ_p is increased. However, once ℓ_p exceeds x_4 (see Fig. 7) the view factor reaches a constant value and remains the same no matter how large the paraboloid

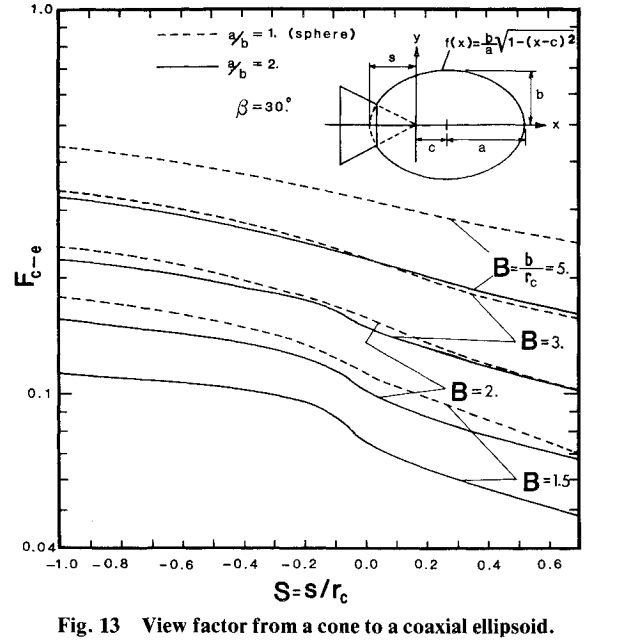

Fig. 13 View factor from a cone to a coaxial ellipsoid.

becomes. If the cone and the paraboloid intersect, the problem reduces to radiation between the truncated cone and a partial paraboloid and, hence involves only regions III and IV. Figure 11 shows a plot of configuration factor against s/r_c with ℓ_1/r_c as a parameter. Similar to the case of radiation between two truncated cones, the view factor attains a maximum value while the cone and the paraboloid are in intersection and the locus of the maximum shifts toward the left for a longer paraboloid.

A study was also done on the effect of the dimensionless eccentricity of the paraboloid a/r_c upon the configuration factor. the results for $S = -1$ and $\beta = 30$ deg are shown in Fig.

12. It is noted that the view factor from cone to paraboloid bears the same characteristic as the view factor from the cone to cone (or truncated cone to truncated cone).

Finally, we will investigate the shape factor from a cone (or a truncated cone) to an ellipsoid (or a partial ellopsoid). The function generator for an elliposid is given by

$$f(x) = (b/a)\sqrt{1-(x-c)^2} \tag{33}$$

where $c=s+a$ and a and b are the half length of the horizontal and vertical axes of the ellipsoid, respectively.

Figure 13 illustrates the variation in the view factor from a cone to an ellipsoid as a function of s/r_c with b/r_c as a parameter. As the ellipsoid continues moving toward the left, the area of the truncated cone becomes smaller and hence the view factor increases. For a fixed value of S, the view factor increases when the dimension b increases, since the chance of radiant beam striking on ellipsoid is higher. The dash line in Fig. 13 represents the case of $a=b$. Under this condition, the ellipsoid becomes a sphere and the corresponding numerical results agree excellently with those given in Ref. 10.

Conclusion

A closed-form solution for a radiative shape factor from a differential element to a cone with an arbitrary angle θ is derived. The limiting solution for which the plane of the element is perpendicular to the axis of the cone, (i.e., $\theta=0$) reduces to the identical mathematical expression obtained earlier by Minning.[6]

Based on the derived formula mentioned above, a general formation is developed for the view factor from a cone to a coaxial axisymmetric body. Numerical results for view factors from cone (or truncated cone) to cone, paraboloid, and ellipsoid are therefore obtained through a single numerical integration instead of the conventional quadruple integration. The only restriction of the present scheme is that the axisymmetric body under consideration cannot block any radiation incident in itself.

Acknowledgment

The work is partially supported by the Research Center of Firestone Tire and rubber Company.

References

[1]Campbell, P. J. and McConnell, D. G., "Radiant Interchange Configuration Factors for Spherical and Conical Surfaces to Spheres," NASA TN D-4457, 1967.

[2]Bobco, R. P., "Radiation from Conical Surfaces with Non-uniform Radiosity," *AIAA Journal*, Vol. 4, March 1966, pp. 544-546.

[3]Edwards, D. K., "Comments on 'Radiation from Conical Surfaces with Non-uniform Radiosity'," *AIAA Journal*, Vol. 7, Aug. 1969, pp. 1656-1659.

[4]Sparrow, E. M., "A New and Simpler Formulation for Radiative Angle Factors," *Journal of Heat Transfer, Transactions of ASME*, Vol. 85, May 1963, pp. 81-88.

[5]Holchendler, J. and Laverty, W. F., "Configuration Factors for Radiant Heat Exchange in Cavities Bounded at the Ends by Parallel Disks and Having Conical Center Bodies," *Journal of Heat Transfer, Transactions of ASME*, Vol. 96, May 1974, pp. 254-257.

[6]Minning, C. P., "Calculation of Shape Factors Between Rings and Inverted Cones Sharing a Common Axis," *Journal of Heat Transfer*, Vol. 99, Aug 1977, pp. 492-494.

[7]Morizumi, S. J., "Analytical Determination of Shape Factors from a Surface Element to an Axisymmetric Surface," *AIAA Journal*, Vol. 2, Aug. 1964, pp. 2028-2030.

[8]Morizumi, S. J., "Analytical Method of Determining Shape Factor from a Surface Element to a Conical Surface," Space Technology Labs Inc., Rept. 62-9721.4-78, 1962.

[9]Kobyshev, A. A., Mastyaeva, I. N. and Surinov, Yu, A., "Study of Radiation Field Created by Conical Radiators," *Soviet Aeronautics*, Vol. 19, 1976, pp. 43-49.

[10]Chung, B.T.F. and Naraghi, M.H.N., "A Simpler Formulation for Radiative View Factors from Spheres to a Class of Axisymmetric Bodies," *Journal of Heat Transfer, Transactions of ASME*, Vol. 104, Feb. 1982, pp. 201-204.

[11]Naraghi, M.H.N. and Chung, B.T.F., "Radiation Configuration Factors between Disks and a Class of Axisymmetric Bodies," *Journal of Heat Transfer, Transactions of ASME*, Vol. 104, Aug. 1982, pp. 426-431.

[12]Howell, J., *Catalog of Radiation Configuration Factors*, McGraw Hill Book Co., New York, 1982.